THERMOPHYSICAL CHARACTERIZATION OF JEZERO CRATER AND NE SYRTIS, MARS. A. Emran[1], L. J. Marzen[1], and D. T. King Jr.[1], [1] Department of Geosciences, Auburn University, 2050 Beard Eaves Coliseum, Auburn, AL 36849. (aze0024@auburn.edu)

Introduction: Jezero crater, with a diameter of 45 km, hosts two inlet channels of deltaic remnants along with an outlet channel and embraces hydrated minerals [1-5]. NE Syrtis (located just south of Jezero crater) has an area of ~ 2500 km^2 and a remarkable mineralogical diversity identified from orbital data as described in Salvatore et al. [6] and references therein. Thermophyscial characteristics are used to quantitatively measure the physical properties of Martian surface [7-11]. These characteristics can be studied through determining thermal inertia (TI), albedo, and diurnal temperature changes on the surface [12-13].

On Mars, thermal inertia is an indicator of surface geological characteristics [14-16]. Surface physical properties, spatial distribution, and transportation of fine materials can be understood from the measurement thermal inertia [17-18]. A lower TI represents unconsolidated loose, fine surface dust, and very few rocks, a medium/intermediate TI means combination of cemented surface, sand sized particles, and a fair number of scattered rocks, whereas a higher TI indicates rocky surface and bedrock outcrops [14-19]. Alternatively, a TI value of <100 Jm^{-2}K^{-1}s$^{-1/2}$ corresponds fine, loosely consolidated material whereas the TI values of >350 Jm^{-2}K^{-1}s$^{-1/2}$ and >1200 Jm^{-2}K^{-1}s$^{-1/2}$ are representative of well-cemented sedimentary rock and crystalline igneous rocks, respectively [20-21]. The albedo is an important component of the total energy balance on Mars by controlling the maximum surface temperature [13,19]. Typically, dust-mantled terrains show high albedo (>0.26) while surfaces with larger grains or rocky materials show relatively low albedo [15-16,18]. This study aimed at determining thermophysical properties of Jezero crater and part of its watershed in NW Isidis and NE Syrtis between ~17^{0}N to 19.5^{0}N and ~76^{0}E to 78.5^{0}E. The objectives of the study are: (a) identifying the distribution of thermal inertia and albedo, and surface geology, and determining the relationship between (b) thermal inertia and albedo, and (c) elevation and thermophysical characteristics.

Methods: Thermal Emission Spectrometer (TES) [22] bolometer data were used to derive thermophysical properties and Mars Orbiter Laser Altimeter (MOLA) derived elevation data. The thermal inertia is produced from nighttime thermal emission measurements of the Martian surface [12-13]. The study used MARSTHERM, a thermophysical analysis tool [23], to derive thermal inertia and albedo using the method developed by Putzig and Mellon [19]. We used bolometer-derived values of TES because of its lower uncertainty and lack of dependence on potentially non-unit emissivity [15-16,19]. This study considered nighttime median rather than mean thermal inertia since seasonal variation in apparent TI can be large and non-linear [19]. Since the surface albedo of Mars changes annually in response to the redistribution dust [24-25], the study considered TES measurement from April 2002 to April 2004. Due to vagueries Mars Global Surveyor (MGS)'s orbital path, few parts of the processing region were un-sampled. We adopted interpolation method of focal analysis (5x5 cell) to fill the missing albedo data. The output was a TES visible-bolometer albedo [22] map at 1/20^0 resolution using the infrared threshold of 0.2 and 0.1, fitting out seasons and locations with high dust and water-ice cloud opacity, respectively [19]. We resampled MOLA elevation data of 128 pixel/degree to 1/20^0 resolution using nearest neighbor algorithm.

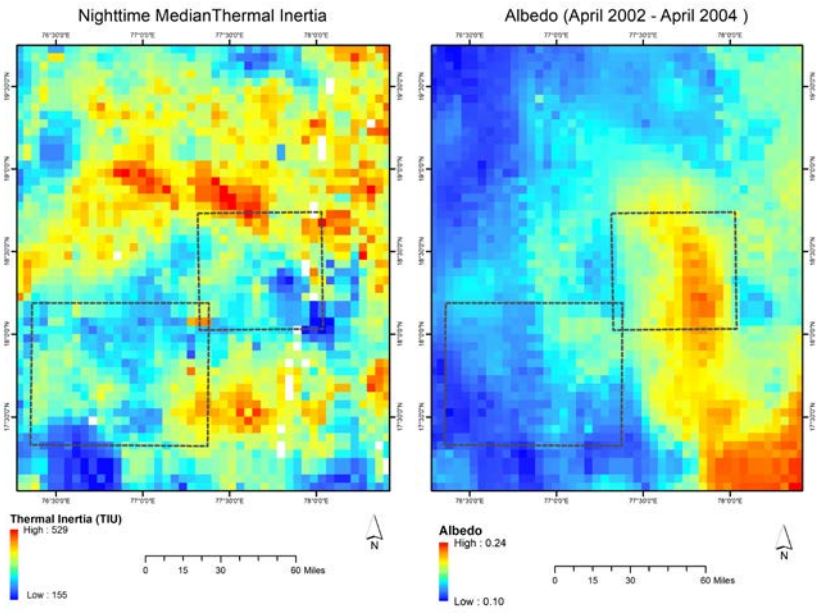

Fig 1: Thermal inertia and albedo distribution on the study area. The black dashed boxes are the location of Jezero crater (upper right) and NE Syrtis (lower left).

Result: *Thernal Intertia-Albedo Distribution and Surface Geology:* The study found thermal inertia of minimum 155 $Jm^{-2}K^{-1}s^{-1/2}$ to maximum 529 $Jm^{-2}K^{-1}s^{-1/2}$ and albedo of minimum 0.10 to maximum 0.24 in processing region. The black dashed boxes in fig. 1 are the location of Jezero crater (upper right) and NE Syrtis (lower left). We found the thermal inertia values of >350 $Jm^{-2}K^{-1}s^{-1/2}$ and the albedo value of ~0.2 (moderately higher thermal inertia/moderate albedo) in the northern and northeastern part of the Jezero crater, particularly around the northern rim and outlet channel part of the crater. The study observed the moderately lower thermal inertia values of <300 $Jm^{-2}K^{-1}s^{-1/2}$ in the southeastern rim of the crater while albedo shows moderately higher values (~0.24). In NE Syrtis, thermal inertia shows a variable pattern whereas albedo has a distinctive pattern of relatively the lower values of <0.15 in most parts and only some moderately lower values of >0.15 in northeastern part. Though the moderately higher values of thermal inertia of >350 $Jm^{-2}K^{-1}s^{-1/2}$ were observed in southeastern parts of NE Syrtis, albedo shows relatively lower values of <0.15. Other parts of NE Syrtis have moderately lower thermal inertia values of <350 $Jm^{-2}K^{-1}s^{-1/2}$ and albedo values of <0.15. It was concluded that the moderate albedo/moderately high inertia in Jezero crater and part of its watershed in NW Isidis and NE Syrtis are probably representative of the cemented sedimentary rock of relatively fine grain size or more-abundant rocks and duricrust, the high albedo/low thermal inertia parts are predominantly of dust mantled terrain, and the low albedo/moderate to high thermal inertia as a windswept, rocky or dust-free surface [15-16,18].

Relationship between TI and Albedo: The study assessed the relationship between TI and albedo using a linear regression analysis considering approximately 500 random points in the processing region. The fitted regression line along with the scatter plot between albedo and TI indicated a very weak positive linear relationship. A unit increase in the thermal inertia there will be approximately 0.0001 unit increase in albedo. The coefficient of determination, R^2 implies the fitted model only explains 3.5% of the total data variation.

Thermophysical Characteristics and Elevation: The relationship between thermophyscial characteristics (thermal inertia and albedo) and topographic parameter of elevation considering the same 500 random sampling points mentioned above was also analyzed. The fitted regression line along with the scatter plot between elevation and thermal inertia indicated negative relationship (very weak). A unit increase in thermal inertia causes approximately 1.7864 unit decrease in elevation. The coefficient of determination, R^2 implies the fitted model explains only 2% of the total data variation. In contrast, the scatter plot between elevation and albedo indicated a high but negative linear relationship. A unit increase in the albedo, the elevation decreases by 14,775 units. The coefficient of determination, R^2 implies the fitted model can explain 55.47% of the total data variation and, therefore, the model is adequate to fit the data.

Conclusion: We found the nighttime median thermal inertia values of 155 - 529 $Jm^{-2}K^{-1}s^{-1/2}$ and the bolometer albedo values of 0.10 - 0.24. Based on the thermophysical characteristics we interpreted the area having a variety of surface materials. Our linear regression analysis shows a very weak positive correlation between albedo and thermal inertia, a very weak negative correlation between elevation and thermal inertia, and a high negative correlation between elevation and albedo.

References: [1] Fassett, C. I. and James W. H. (2005) *GRL*, 32 (14), L14201. [2] Ehlmann, B. L. et al. (2008) *Nature Geoscience*, 1 (6), ngeo207. [3] Ehlmann, B. L. et al. (2009) *JGR*, 114 (E2), E00D08. [4] Goudge, T. A. et al. (2015) *JGR*, 120 (4), 2014JE004782. [5] Schon, S. C. et al. (2012) *Planetary and Space Science*, 67 (1), 28–45. [6] Salvatore, M. R. et al. (2017) *Icarus*, 301, 76-96. [7] Kieffer, H. H. et al. (1973) *JGR*, 78 (20), 4291–4312. [8] Jakosky, B. M. (1986) *Icarus*, 66 (1), 117–24. [9] Presley, M. A. and Christensen, P.R. (1997) *JGR*, 102 (E3), 6535–49. [10] Presley, M. A. and Christensen, P.R. (1997) *JGR*, 102 (E3), 6551–66. [11] Piqueux, S. and Christensen, P.R. (2011) *JGR*, 116 (E7), E07004. [12] Jakosky, B.M. et al. (2006) *JGR*, 111 (E8), E0800. [13] Murphy, N. W. et al. (2007) *JGR*, 112 (E5), E05004. [14] Jakosky, B. M. et al. (2000) *JGR*, 105 (E4), 9643–52. [15] Mellon, M.T. et al. (2000) *Icarus*, 148 (2), 437–55. [16] Putzig, N. E. et al. (2005) *Icarus*, 173 (2), 325–41. [17] Kieffer, H. H. et al. (1977) *JGR*, 82 (28), 4249–91. [18] Palluconi, F. D. and Kieffer, H.H. (1981) *Icarus*, 45 (2), 415–26. [19] Putzig, N.E. and Mellon, M.T. (2007) *Icarus*, 191 (1), 68–94. [20] Edwards, C. S. et al. (2009) *JGR*, 114 (E11), E11001. [21] Fraeman, A. A. et al. (2016) *JGR*, 121 (9), 2016JE005095. [22] Christensen, P. R. et al. (2001) *JGR*, 106 (E10), 23823–71. [23] Putzig, N.E. et al. (2013) *AGU*, Abstract #P43C-2023. [24] Pleskot, L. K. and Miner, E. D. (1981) *Icarus*, 45 (1), 179–201. [25] Christensen, P. R. (1988) *JGR*, 93 (B7), 7611–24.